be essential for state 1–state 2 transitions, which regulate energy transfer from phycobilisomes to photosystem II and photosystem I over a timescale of seconds to minutes[14,19]. State transitions have been proposed to involve the decoupling of phycobilisomes from photosystem II and binding to photosystem I[14,19–21]. Our results suggest that the phycobilisomes are the mobile element. A calculation based on our measured diffusion coefficients indicates that the diffusion of phycobilisomes from photosystem II to photosystem I could be complete within 100 ms. The rate of state transitions could be limited by the signal transduction pathway rather than the diffusion of the phycobilisomes. □

Methods

Growth and preparation of cells. *Dactylococcopsis salina*[8] was grown at 30 °C and with moderate illumination in liquid growth medium[8]. Cells were spread on 0.6% agar containing the same growth medium, covered with a 0.2-mm quartz coverslip and placed on a stage heated to 30 °C under the microscope objective. The objective was immersed in a drop of glycerol on the coverslip.

FRAP measurement. We used the scanning confocal microscope Syclops[22] at the Daresbury Laboratory. The lasers used were He–Ne (633 nm, 150 mW) or He–Cd (442 nm, 60 mW). The laser light was focused, passed through a 15-μm pinhole and focused onto the sample with a 100× objective lens. The vertical (Z) resolution was 2.6 μm (FWHM) and the resolution in the x–y plane was about 0.32 μm with 633-nm light, and 0.23 μm with 442 nm light (FWHM). The laser was scanned over the sample with oscillating mirrors. Fluorescence from the sample was separated from the excitation light with a polarizing beamsplitter and long-pass filters (Schott RG665), passed through a 40-μm pinhole and detected with a cooled photomultiplier (Hamamatsu R3896). The sample was bleached by scanning the laser repeatedly in one dimension across the cell for 20 s. The laser power was then reduced tenfold with a neutral density filter and the cell was imaged by scanning over a square of 75 × 75 μm in the x–y plane. There was no detectable photobleaching during the recording of successive image scans.

Data analysis. Fluorescence images were aligned and an image recorded before the bleach was subtracted. A one-dimensional bleaching profile was extracted (Fig. 1) using Optimas image analysis software (Optimas Corporation). To extract the width and depth of the bleach, the bleaching profile was fitted as a gaussian curve using Sigmaplot (Jandel Scientific).

Received 3 July; accepted 4 September 1997.

1. Krauss, N. *et al.* Photosystem I at 4-Å resolution represents the first structural model of a joint photosynthetic reaction centre and core antenna system. *Nature Struct. Biol.* **3,** 965–973 (1996).
2. Sidler, W. A. in *The Molecular Biology of Cyanobacteria* (ed. Bryant, D. A.) 139–216 (Kluwer Academic, Dordrecht, 1994).
3. McDermott, G. *et al.* Crystal structure of an integral membrane light-harvesting complex from photosynthetic bacteria. *Nature* **374,** 517–521 (1995).
4. Kühlbrandt, W., Wang, D. N. & Fijiyoshi, Y. Atomic model of plant light-harvesting complex by electron crystallography. *Nature* **367,** 614–621 (1994).
5. Holzenburg, A., Bewley, M. C., Wilson, F. H., Nicholson, W. V. & Ford, R. C. Three-dimensional structure of photosystem II. *Nature* **363,** 470–473 (1993).
6. Boekema, E. J. *et al.* Supramolecular structure of the photosystem II complex from green plants and cyanobacteria. *Proc. Natl Acad. Sci. USA* **92,** 175–179 (1995).
7. Thomas, J. & Webb, W. W. in *Non-invasive Techniques in Cell Biology* 129–152 (Wiley–Liss, New York, 1990).
8. Walsby, A. E., van Rijn, J. & Cohen, Y. The biology of a new gas-vacuolate cyanobacterium, *Dactylococcopsis salina* sp. nov. in Solar Lake. *Proc. R. Soc. Lond. B* **217,** 417–447 (1983).
9. Zhang, F., Lee, G. M. & Jacobson, K. Protein lateral mobility as a reflection of membrane microstructure. *BioEssays* **15,** 579–588 (1993).
10. Kubitscheck, U., Wedekind, P. & Peters, R. Lateral diffusion measurement at high spatial resolution by scanning microphotolysis in a confocal microscope. *Biophys. J.* **67,** 948–956 (1994).
11. Drepper, F., Carlberg, I., Andersson, B. & Haehnel, W. Lateral diffusion of an integral membrane protein: Monte Carlo analysis of the migration of phosphorylated light-harvesting complex II in the thylakoid membrane. *Biochemistry* **32,** 11915–11922 (1993).
12. Barber, J. & Andersson, B. Revealing the blueprint of photosynthesis. *Nature* **370,** 31–34 (1994).
13. Holzwarth, A. R. Fluorescence lifetimes in photosynthetic systems. *Photochem. Photobiol.* **43,** 707–725 (1986).
14. Bald, D., Kruip, J. & Rögner, M. Supramolecular architecture of cyanobacterial thylakoid membranes: how is the phycobilisome connected with the photosystems? *Photosynth. Res.* **49,** 103–118 (1996).
15. Giddings, T. H., Wasmann, C. & Staehelin, L. A. Structure of the thylakoids and envelope membranes of the cyanelles of *Cyanophora paradoxa*. *Plant Physiol.* **71,** 409–419 (1983).
16. Mustardy, L., Cunningham, F. X. & Gantt, E. Photosynthetic membrane topography: quantitative *in situ* localisation of photosystems I and II. *Proc. Natl Acad. Sci. USA* **89,** 10021–10025 (1992).
17. Adir, N., Shochat, S. & Ohad, I. Light-dependent D1 protein synthesis and translocation is regulated by reaction centre II. *J. Biol. Chem.* **265,** 12563–12568 (1990).
18. Allen, J. F. Protein phosphorylation in regulation of photosynthesis. *Biochim. Biophys. Acta* **1098,** 275–335 (1992).
19. Soitamo, A. J. *et al.* Overproduction of the D1:2 protein makes *Synechococcus* cells more tolerant to photoinhibition of photosystem II. *Plant Mol. Biol.* **30,** 467–478 (1996).
20. Mullineaux, C. W., Bittersmann, E., Allen, J. F. & Holzwarth, A. R. Picosecond time-resolved fluorescence emission spectra indicate decreased excitation energy transfer from the phycobilisome to photosystem II in the cyanobacterium *Synechococcus* 6301. *Biochim. Biophys. Acta* **1015,** 231–242 (1990).
21. Mullineaux, C. W. Excitation energy transfer from phycobilisomes to photosystem I in a cyanobacterial mutant lacking photosystem II. *Biochim. Biophys. Acta* **1184,** 71–77 (1994).
22. van der Oord, C. J. R. *et al.* High-resolution confocal microscopy using synchrotron radiation. *J. Microsc.* **182,** 217–224 (1996).

Acknowledgements. We thank A. E. Walsby for discussion and for the culture of *Dactylococcopsis salina*.

Correspondence and requests for materials should be addressed to C.W.M. (e-mail: c.mullineaux@ucl.ac.uk).

corrections

NMR structure of a receptor-bound G-protein peptide

Edward A. Dratz, Julie E. Furstenau, Christophe G. Lambert, Dennis L. Thireault, Helen Rarick, Theresa Schepers, Sergei Pakhlevaniants & Heidi E. Hamm

Nature **363,** 276–280 (1993)

In this Letter we reversed the assignment of the amino proton resonances of 8HN (Cys 347) and 11HN (Phe 350), as pointed out by J. Russo and L. M. Gierasch (personal communication). This correction caused some alterations in the preferred structures at the same level of refinement as used in our Letter; however, further refinement has led to additional alterations in the receptor-bound structures. Some of the peptide-transferred NOESY NMR intensities showed evidence for mediation by rhodopsin protons at higher levels of structure refinement, as supported by spin-echo filtering of the rhodopsin magnetization during the Tr-NOESY mixing time. Protons on the large protein that are in intimate contact with the ligand can mediate ligand proton cross-relaxation and distort the apparent distances between ligand protons. Partial compensation for rhodopsin mediation of peptide Tr-NOESY, by spin-echo filtering, led to further alterations of the structures and considerable improvement of the agreement of the bound peptide structures with the data[1]. More quantitative estimation of receptor mediation of peptide Tr-NOESY and refined structures of receptor-bound G-protein peptides will be published later. □

1. Dratz, E. A., Gizachew, D., Busse, S. C., Rens-Domiano, S. & Hamm, H. E. NMR structure of a receptor bound G protein peptide: Structure refinement and update *Biophys. J.* **70,** *A*16 (1996).

DNA antisense therapy for asthma in an animal model

Jonathan W. Nyce & W. James Metzger

Nature **385,** 721–725 (1997)

It has come to our attention that this Letter contains the following errors, none of which changes the substance of the findings or the interpretation of the data. (1) The sequence given for the bradykinin B_2 mismatch molecule (B_2MM) contains a gap—it should read 5′-GGT GAT CTT GAG GAT TTC GGC-3′; (2) in the Methods section labelled "Receptor binding", all dosages of antisense are indicated as 0.2 mg, whereas they should read 0.2 mg, 2.0 mg and 20.0 mg for each oligonucleotide tested; and (3) Scatchard plots of saturation isotherms were misdrawn; the correct K_d and B_{max} values are found in Table 1. □

plants. Although the significance of MeSA-mediated communication among field grown-plants is unknown, MeSA may accumulate inside dense canopies and exert a physiological effect. □

Methods

Extraction and quantification of SA. Tobacco (*Nicotiana tabacum* cv Xanthinc) seeds were germinated and grown as described[20]. Total SA (sum of free and glucosylsalicylic acid) was measured following the hydrolysis of leaf (0.5 g fresh weight) extracts with almond β-glucosidase (Sigma)[26]. SA concentrations in hydrolysed extract were determined by spectrofluorescence using HPLC[15]. All data were corrected for SA recovery.

Quantification of MeSA. Five-week-old tobacco plants were inoculated on two middle leaves with the U1 strain of TMV[20] and placed into a 1-l Wheaton purge-and-trap apparatus (Wheaton). Air filtered through activated charcoal was passed through the apparatus (40 ml per min flow rate) and volatiles were collected in a silylated glass-lined stainless-steel desorption tube (3.0 mm i.d. × 10 mm length; Scientific Instrument Services) packed with 100 mg of Tenax-TA resin (60/80 mesh; Scientific Instrument Services). D8-naphthalene was added to the absorbent traps as an internal standard. Trapped volatiles were analysed using a short-path thermal desorption system[27] (Scientific Instrument Services) connected to the injection port of a Varian 3040 gas chromatograph equipped with DB-5MS capillary column connected by a heated transfer line maintained at 280 °C to the ion source of a Finnigan-MAT 8230 high-resolution double-focusing magnetic sector mass spectrometer[21].

Liquid chromatography and mass spectrometry. LC-MS analysis was done on a Micromass Platform II LC-MS (Micromass, Altringham, UK) using negative ion atmosphere pressure chemical ionization (APCI). Cone voltage was 15 V and there was little or no fragmentation of molecular anions; source temperature was 150 °C and the APCI probe temperature was 350 °C. Data were analysed using Masslinx v.2.0 software.

RNA isolation and blot hybridization analysis. Tobacco PR-1 mRNA was detected with a radioactive probe prepared from the PR-1 cDNA by random priming (gift from E. Ward). Total leaf RNA (30 μg) was loaded in each lane and PR-1 transcripts were detected with tobacco PR-1 cDNA. As a loading control, blots were stripped and rehybridized with a probe for 18S rRNA (gift from R. Mittler).

Received 23 September; accepted 12 December 1996.

1. Buttery, R. G., Ling, L. C. & Wellso, S. G. *J. Agr. Food Chem.* **30,** 791–792 (1982).
2. Buttery, R. G., Kamm, J. A. & Ling, L. C. *J. Agr. Food Chem.* **32,** 254–256 (1984).
3. Buttery, R. G., Flath, R. A., Mon, T. R. & Ling, L. C. *J. Agr. Food Chem.* **34,** 820–822 (1986).
4. Kobayashi, A., Kubota, K. & Yano, M. in *Bioactive Volatile Compounds from Plants* (eds Teranishi, R., Buttery, R. G. & Sugisawa, H.) 49–56 (Am. Chem. Soc., Washington, 1993).
5. Buttery, R. G. & Ling, C. in *Bioactive Volatile Compounds from Plants* (eds Teranishi, R., Buttery, R. G. & Sugisawa, H.) 23–34 (Am. Chem. Soc., Washington, 1993).
6. Anderson, R. A. *et al. J. Agr. Food Chem.* **36,** 295–299 (1988).
7. Hill, N. G., Williams, N. H. & Dodson, C. H. *Biotropica* **4,** 61–68 (1972).
8. Dicke, M. *et al. J. Chem. Ecol.* **16,** 381–396 (1990).
9. Dicke, M., Sabelis, M. W., Takabayashi, J., Bruin, J. & Posthumus, M. A. *J. Chem. Ecol.* **16,** 3091–3118 (1990).
10. Ryals, J., Uknes, S. & Ward, E. *Plant Physiol.* **104,** 1109–1112 (1994).
11. Carr, J. P. & Klessig, D. F. in *Genetic Engineering, Principles and Methods* Vol. 11 (ed. Setlov, J. K.) 65–109 (Plenum, New York and London, 1989).
12. Malamy, J., Carr, J. P., Klessig, D. F. & Raskin, I. *Science* **250,** 1002–1004 (1990).
13. Malamy, J., Hennig, J. & Klessig, D. F. *Plant Cell* **4,** 359–366 (1992).
14. Kassanis, B. *Ann. Appl. Biol.* **39,** 358–369 (1952).
15. Leon, J., Yalpani, N., Raskin, I. & Lawton, M. A. *Plant Physiol.* **103,** 323–328 (1993).
16. Hamilton-Kemp, T. R. *et al. J. Chem. Ecol.* **14,** 789–796 (1988).
17. Robertson, G. W., Griffiths, D. W., MacFarlane Smith, W. & Batcher, R. D. *Phytochem. Anal.* **4,** 152–157 (1993).
18. Muller, S., Efer, J. & Engewald, W. *Chromatographia* **38,** 694–700 (1994).
19. Enyedi, A. J., Yalpani, N., Silverman, P. & Raskin, I. *Cell* **70,** 879–886 (1992).
20. Yalpani, N., Silverman, P., Wilson, T. M. A., Kleier, D. A. & Raskin, I. *Plant Cell* **3,** 809–818 (1991).
21. Shulaev, V., Leon, J. & Raskin, I. *Plant Physiol.* **103,** 315–321 (1993).
22. Yalpani, N., Leon, J., Lawton, M. A. & Raskin, I. *Plant Physiol.* **103,** 315–321 (1993).
23. Rasmussen, J. B., Hammerschmidt, R. & Zook, M. N. *Plant Physiol.* **97,** 1342–1347 (1991).
24. Ryals, J., Uknes, S. & Ward, E. *Plant Physiol.* **104,** 1109–1112 (1994).
25. Guedes, M. E. M., Richmond, S. & Kuc, J. *Physiol. Plant Path.* **17,** 229–233 (1980).
26. Enyedi, A. J., Yalpani, N., Silverman, P. & Raskin, I. *Proc. Natl Acad. Sci. USA* **89,** 2480–2484 (1992).
27. Hartman, T. G. *et al.* in *Flavor Measurements* (eds Ho, C.-T. & Manley, C. H.) 37–60 (Dekker, New York, Basel and Hong Kong, 1993).

Acknowledgements. We thank E. Ward for the PR-1 cDNA clone, R. Mittler for the 18S rRNA probe, and I. Chet, P. Day, M. A. Lawton, R. Mittler, M. Moynihan and R. Smith for discussion.

Correspondence and requests for materials should be addressed to I.R. (e-mail: raskin@aesop.rutgers.edu).

DNA antisense therapy for asthma in an animal model

Jonathan W. Nyce*† **& W. James Metzger**‡

* *Department of Molecular Pharmacology and Therapeutics, EpiGenesis Pharmaceuticals, Greenville, North Carolina 27834, USA*
‡ *Department of Medicine, Section of Allergy, Asthma and Immunology, and* † *Department of Pharmacology, School of Medicine, East Carolina University, Greenville, North Carolina 27858, USA*

Asthma is an inflammatory disease characterized by bronchial hyper-responsiveness that can proceed to life-threatening airway obstruction. It is one of the most common diseases in industrialized countries, and in the United States accounts for about 1% of all healthcare costs[1]. Asthma prevalence and mortality have increased dramatically over the past decade[2], and occupational asthma is predicted to be the pre-eminent occupational lung disease in the next decade[3]. Increasing evidence suggests that adenosine, an endogenous purine that is involved in normal physiological processes, may be an important mediator of bronchial asthma[4–15]. In contrast to normal individuals, asthmatic individuals respond to adenosine challenge with marked airway obstruction[6,7], and concentrations of adenosine are elevated in the bronchoalveolar lavage fluid of asthma patients[9]. We performed a randomized crossover study using the dust mite-conditioned allergic rabbit model of human asthma. Administration of an aerosolized phosphorothioate antisense oligodeoxynucleotide targeting the adenosine A_1 receptor desensitized the animals to subsequent challenge with either adenosine or dust-mite allergen.

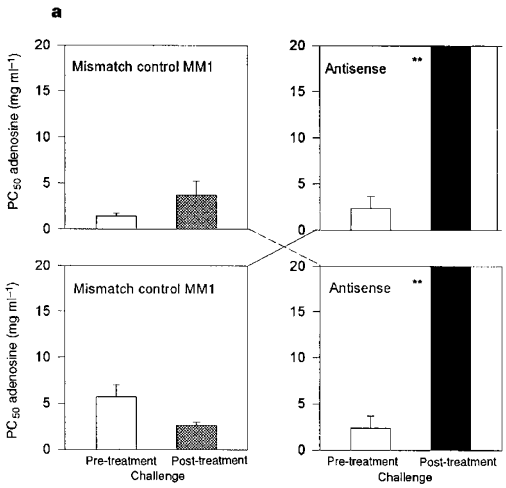

b

PC_{50} Adenosine					
A_1 MM Control		A_1 MM2 control		A_1AS	
Pre ODN	Post ODN	Pre ODN	Post ODN	Pre ODN	Post ODN
3.56 ± 1.02	3.25 ± 0.34	2.46 ± 0.50	2.81 ± 0.70	2.36 ± 0.68	>19.5 ±0.34**

Figure 1 a, Effects of adenosine A_1 receptor antisense ODN upon PC_{50} values in asthmatic rabbits. PC_{50} adenosine values were determined before and after intratracheal administration of aerosolized A_1AS or A_1MM to allergic rabbits. After a two-week rest period between parts of the experiment, rabbits were then crossed over, with those that had received A_1AS in the first part now receiving A_1MM, and those that had received A_1MM in the first part now receiving A_1AS. A_1MM2-treated animals were a separate group. **b**, Data summary. Results are presented as the mean ± s.e.m. Significance was determined by repeated-measures ANOVA and Tukey's protected *t*-test. Asterisks indicate a significant difference from all other groups, $P < 0.01$.

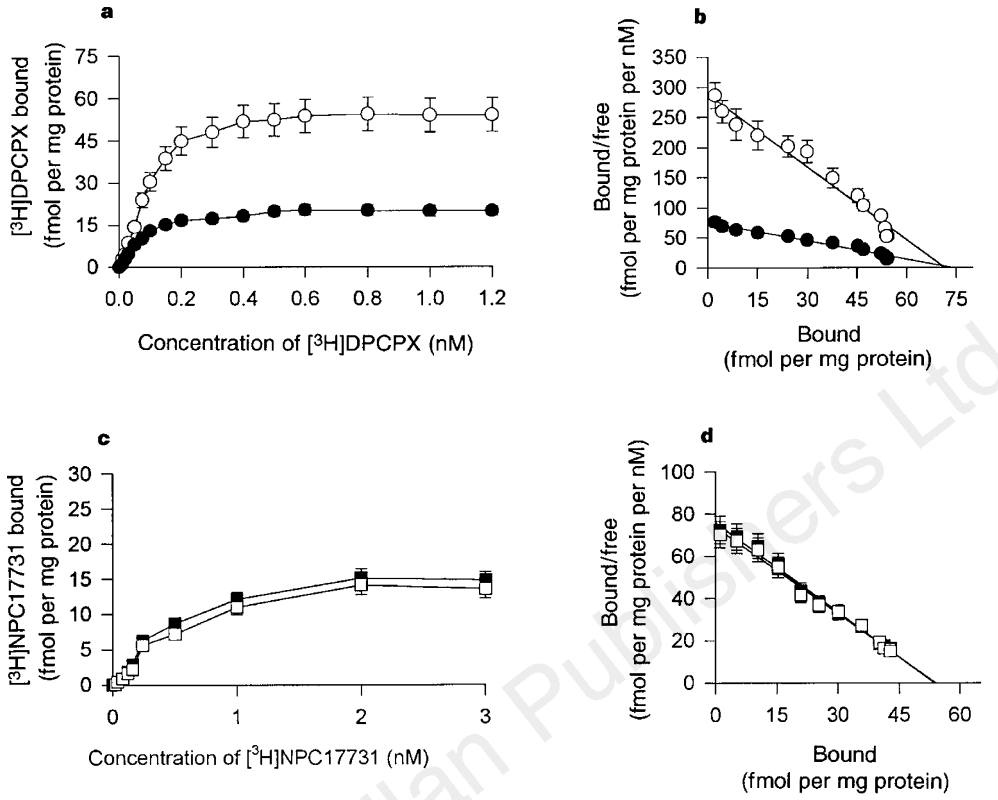

Figure 2 Specificity of action of adenosine A_1 receptor antisense ODN A_1AS. Airway smooth muscle tissue was dissected from rabbits administered a total of 20 mg A_1AS or A_1MM in four divided doses over 48 h. Plasma-membrane fractions were prepared. **a**, Saturation isotherm of [^{3}H]DPCPX binding to allergic rabbit lung plasma membrane from A_1AS- (filled circles) and A_1MM-treated (open circles) allergic rabbits showing an approximate 75% decrease in adenosine A_1 receptor number in airway smooth muscle from A_1AS-treated animals. **b**, Scatchard plot of saturation isotherm from **a** indicating a single class of binding sites; A_1AS (filled circles), A_1MM (open circles). **c**, Saturation isotherm of [^{3}H] NPC17731 binding to allergic rabbit lung plasma membrane from A_1AS- (open squares) and A_1MM-treated (filled squares) allergic rabbits showing no change in bradykinin B_2 receptor number in airway smooth muscle of A_1AS-treated animals. **d**, Scatchard plot of saturation isotherm from **c** indicating a single class of binding sites. A_1AS (open squares), A_1MM (filled squares). Error bars represent s.e.m.

Antisense oligodeoxynucleotides (ODNs) induce functional gene ablation by degenerating the template activity of specific target mRNAs[16,17]. We considered the lung to represent an excellent potential target for aerosolized antisense ODNs, for several reasons. The lung can be approached non-invasively and relatively specifically by inhaled aerosolized ODNs; it has a very large absorption surface (150 m^2 in the human); and it is lined with surfactant, a material that could potentially facilitate the pulmonary distribution and intracellular uptake of respired ODNs. In this regard, cationic lipids have been used to enhance cellular uptake of antisense ODNs[18,19], and dipalmitoylphosphatidylcholine, a major constituent of surfactant, is a zwitterionic lipid that can act as a weak cation at physiological pH. Indeed, a surfactant-based delivery system for transfection of airway cells with DNA has been described[20]. Other aspects of the physiology of surfactant, for example its high rate of recycling between the alveolar surface and the pulmonary epithelium[21], might also potentially facilitate pulmonary distribution and uptake of respired ODNs. We considered bronchial hyperresponsiveness in the allergic rabbit model of human asthma to be an excellent endpoint for antisense application because the tissues involved in this response lie near the point of contact with aerosolized ODNs, and the model closely simulates an important human disease. Furthermore, a serendipitous homology between the human and rabbit adenosine A_1 receptors centring on the initiation codon allowed us to use in the allergic rabbit model an antisense ODN (A_1AS) designed to target the human adenosine A_1 receptor mRNA.

In the first part of the experiment, four randomly selected allergic rabbits were administered A_1AS, and four were administered a mismatched control, A_1MM. On the morning of the third day, PC_{50} values (the concentration of aerosolized adenosine required to reduce the dynamic compliance of the bronchial airway 50% from the baseline value) were obtained and compared with PC_{50} values obtained for these animals before exposure to ODN. The experiment was repeated two weeks later in crossover fashion, with the animals previously treated with A_1AS now receiving the mismatched control A_1MM, and the animals previously treated with A_1MM now receiving A_1AS. Another group of four animals was administered a second mismatch control, A_1MM2. The results of this experiment are shown in Fig. 1. In both parts of the experiment, animals receiving the antisense ODN showed an increase of at least an order of magnitude in the dose of aerosolized adenosine required to reduce dynamic compliance of the lung by 50%. No effect of the mismatched control ODNs upon PC_{50} values was observed. A_1AS desensitized allergic rabbits to adenosine in a dose-dependent fashion over a range of 0.2, 2.0 and 20.0 mg total dose, and A_1MM was without effect over this same dose range.

When the crossover experiment was completed, airway smooth muscle was surgically dissected from all of the rabbits and processed for quantitative assessment of adenosine A_1 receptors. As a control for specificity of the antisense ODN, adenosine A_2 receptors and bradykinin B_2 receptors were also quantified. Rabbits treated with A_1AS in the crossover experiment had a nearly 75% decrease in A_1

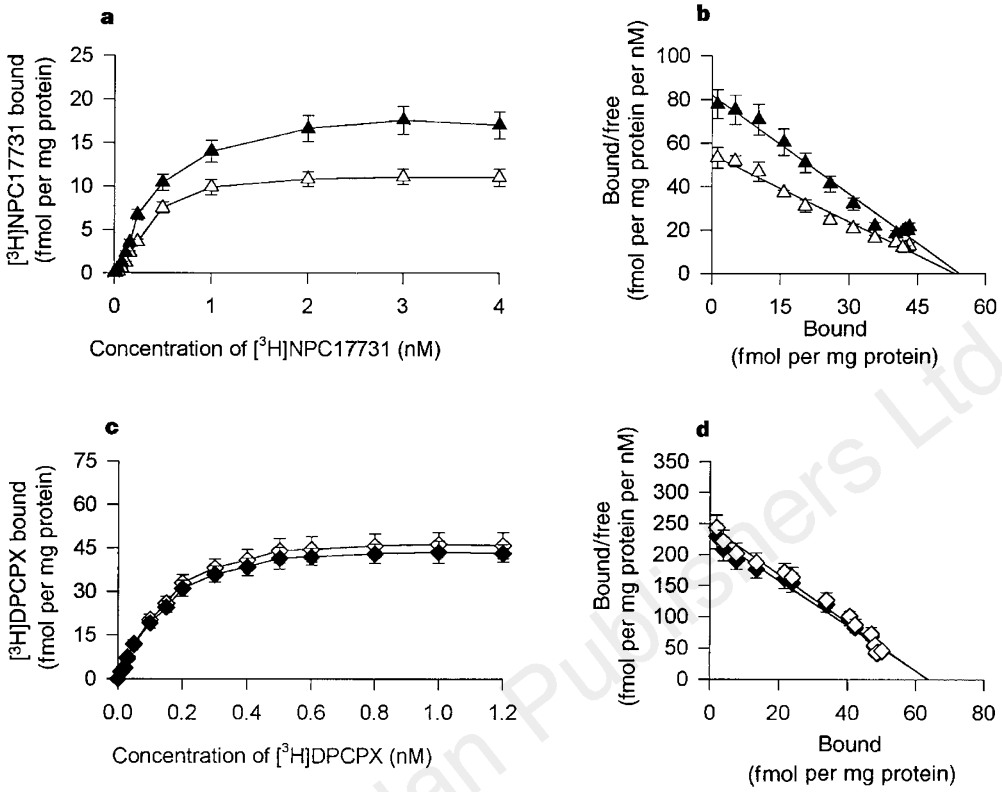

Figure 3 Specificity of action of bradykinin B_2 receptor antisense ODN B_2AS. Airway smooth muscle tissue was dissected from rabbits administered 20 mg B_2AS or B_2MM in four divided doses over 48 h. Plasma-membrane fractions were prepared. **a**, Saturation isotherm of [^{3}H]NPC17731 binding to allergic rabbit lung plasma membrane from B_2AS- (open triangles) and B_2MM-treated (filled triangles) allergic rabbits showing an approximate 40% decrease in bradykinin B_2 receptor number in airway smooth muscle from B_2AS-treated animals. **b**, Scatchard plot of saturation isotherm from **a** indicating a single class of binding sites; B_2AS (open triangles), B_2MM (filled triangles). **c**, Saturation isotherm of [^{3}H]DPCPX binding to allergic rabbit lung plasma membrane from B_2AS- (open diamonds) and B_2MM-treated (filled diamonds) allergic rabbits showing no change in adenosine A_1 receptor number. **d**, Scatchard plot of saturation isotherm from **c** indicating a single class of binding sites; B_2AS (open diamonds), B_2MM (filled diamonds).

receptor density compared with controls (Fig. 2), as assayed by specific binding of [^{3}H]-DPCPX. This effect occurred in a dose-dependent fashion over the range 0.2, 2.0 and 20.0 mg total dose. There was no change in adenosine A_2 receptor density, as assayed by specific binding of the A_2 receptor-specific ligand 2-[-p(2-carboxyethyl) - phenethylamino] - 5′- (N - ethylcarboxamido) adenosine (CGS-21680), or in bradykinin B_2 receptor density, as assayed by specific binding of the bradykinin B_2 receptor-specific ligand NPC17731, over this same dose range of A_1AS. Scatchard analysis of the binding isotherm of [^{3}H]-DPCPX to membranes prepared from bronchial smooth muscle isolated from allergic rabbits treated with 20 mg A_1AS yielded K_d and B_{max} values of 0.36 nM and 19 fmol mg^{-1} protein, respectively, compared with values of 0.34 nM and 52 fmol mg^{-1} protein, respectively, for rabbits treated with control A_1MM ODN (Fig. 2). This confirms that there is effective and selective attenuation by A_1AS of a single class of adenosine receptors of the A_1 type.

As a further control to demonstrate gene-specific effects in this model system, an antisense ODN targeting the bradykinin B_2 receptor (B_2AS) was administered as an aerosol to allergic rabbits under the same conditions as for A_1AS. Like adenosine, bradykinin is a potent bronchoconstrictor agent in asthmatic airways[22], and this effect is thought to be mediated through the B_2 receptor[23,24]. Aerosolized B_2AS specifically downregulated B_2 receptor binding by the B_2 receptor-specific ligand [^{3}H]-NPC17731 in airway smooth muscle of allergic rabbits (Fig. 3a, b). Neither adenosine A_1 nor A_2 receptor binding by their specific ligands was affected by B_2AS over the dose range 0.2, 2.0 and 20.0 mg. A minimally mismatched control molecule, B_2MM, was without effect on any receptor over this same dose range. Scatchard analysis of the binding isotherm of [H^3]-NPC17731 to membranes prepared from bronchial smooth muscle isolated from allergic rabbits treated with 20 mg B_2AS yielded K_d and B_{max} values of 0.38 nM and 8.7 fmol mg^{-1} protein, respectively, compared with values of 0.41 nM and 14.0 fmol mg^{-1} protein, respectively, for rabbits treated with control B_2MM ODN (Fig. 3). This confirms that there is specific attenuation by B_2AS of a single class of receptors of the B_2 type.

These results show that aerosolized A_1AS reached airway smooth muscle; reduced adenosine A_1 receptor number in this tissue in a dose-dependent manner; had no effect on either the adenosine A_2 or bradykinin B_2 receptors; and attenuated the bronchoconstrictor response to adenosine challenge in allergic rabbits. B_2AS provided further evidence of selective attenuation of target gene expression in this system, as it reduced bradykinin B_2 receptor number in airway smooth muscle in a dose-dependent manner, and was without effect on adenosine A_1 or A_2 receptors. Furthermore, all three mismatch control molecules (A_1MM, A_1MM2 and B_2MM), each minimally different from their corresponding antisense molecules, were completely without effect at any receptor at every dose tested. These results provide a clear demonstration of gene-specific antisense effects by aerosolized ODNs in the asthmatic rabbit lung (Table 1).

To assess further the role of the adenosine A_1 receptor in

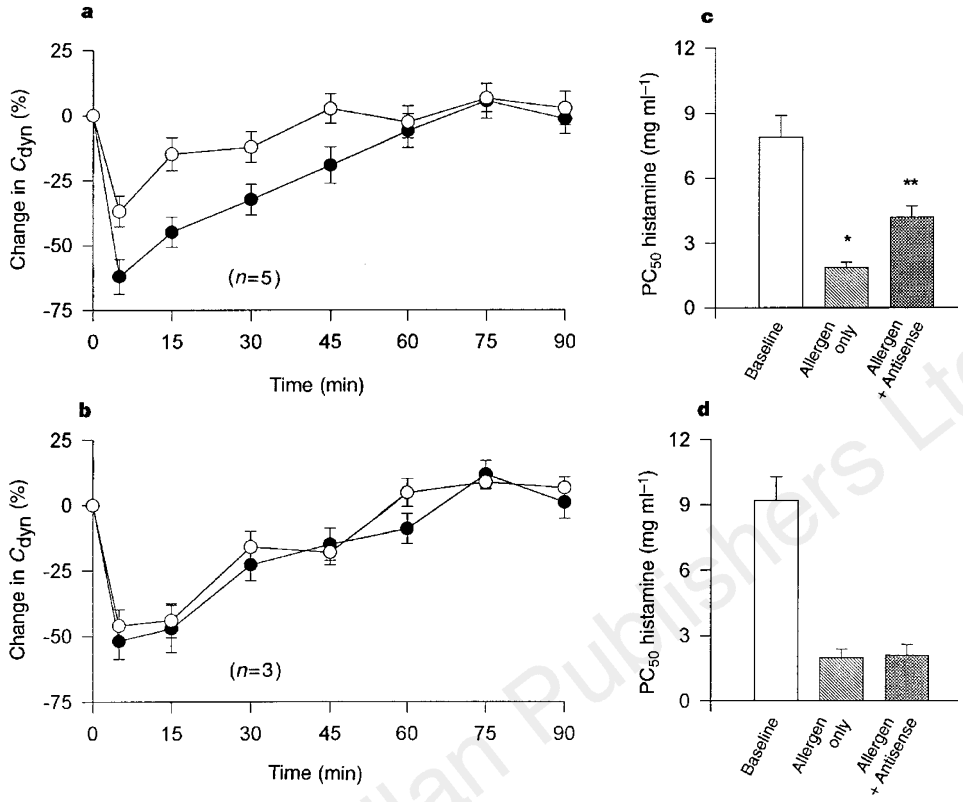

Figure 4 The effect of antisense and mismatch ODNs on allergen-induced airway obstruction and bronchial hyperresponsiveness in allergic rabbits. **a**, Effect of A_1AS antisense ODN on allergen-induced airway obstruction. Allergen only (filled circles); allergen + antisense (open circles). As calculated from the area under the curve, A_1AS significantly inhibited allergen-induced airway obstruction (55%, $P < 0.05$; repeated measures ANOVA and Tukey's *t*-test. **b**, Lack of effect of mismatch control A_1MM on allergen-induced airway obstruction. Allergen only (filled circles); allergen + antisense (open circles). **c**, Effect of A_1AS antisense ODN on allergen-induced bronchial hyperresponsiveness. As calculated from the PC_{50} histamine, A_1AS significantly inhibited allergen-induced bronchial hyperresponsiveness in allergic rabbits (61%, $P < 0.05$; repeated measures ANOVA and Tukey's *t*-test). **d**, Lack of effect of A_1MM mismatch control on allergen-induced bronchial hyperresponsiveness. Dynamic compliance (C_{dyn}) is the change in the volume of the lungs divided by the change in the alveolar-distending pressure during the course of a breath.

Table 1 Binding characteristics

Treatment	A_1 receptor		B_2 receptor	
A_1AS (mg)	K_d (nM)	B_{max} (fmol)	K_d (nM)	B_{max} (fmol)
20	0.36 ± 0.029	19 ± 1.52*	0.39 ± 0.031	14.8 ± 0.99
2	0.38 ± 0.030	32 ± 2.56*	0.41 ± 0.028	15.5 ± 1.08
0.2	0.37 ± 0.030	49 ± 3.43	0.34 ± 0.024	15.0 ± 1.06
A_1MM (mg)				
20	0.34 ± 0.027	52.0 ± 3.64	0.35 ± 0.024	14.0 ± 1.0
2	0.37 ± 0.033	51.8 ± 3.88	0.38 ± 0.028	14.6 ± 1.02
0.2	0.39 ± 0.027	48.3 ± 2.92	0.40 ± 0.032	15.7 ± 1.35
B_2AS (mg)				
20	0.36 ± 0.028	45.0 ± 3.15	0.38 ± 0.027	8.7 ± 0.62*
2	0.39 ± 0.035	44.3 ± 2.90	0.34 ± 0.024	11.9 ± 0.76**
0.2	0.40 ± 0.028	47.0 ± 3.76	0.35 ± 0.028	15.1 ± 1.05
B_2MM (mg)				
20	0.39 ± 0.031	42.0 ± 2.94	0.41 ± 0.029	14.0 ± 0.98
2	0.41 ± 0.035	40.0 ± 3.20	0.37 ± 0.030	14.8 ± 0.99
0.2	0.37 ± 0.029	43.0 ± 3.14	0.36 ± 0.025	15.1 ± 1.35
Saline control	0.37 ± 0.041	46.0 ± 5.21	0.39 ± 0.047	14.2 ± 1.35

Binding characteristics of the adenosine A_1-selective ligand [^{3}H]DPCPX and the bradykinin B_2-selective ligand [^{3}H]NPC 17731 in membranes isolated from airway smooth muscle of A_1 adenosine receptor and B_2 bradykinin receptor antisense- and mismatch-treated allergic rabbits. Treatment values refer to total ODN administered in four equivalently divided doses over a 48-h period. Significance was determined by repeated-measures ANOVA and Tukey's protected *t*-test; $N = 4$–6 for all groups. All assays were performed in triplicate.
* Significantly different from mismatch control- and saline-treated groups, $P < 0.001$.
** Significantly different from mismatch control- and saline-treated groups, $P < 0.05$.

mediating airway obstruction and bronchial hyperresponsiveness, allergic rabbits were administered A_1AS or control A_1MM followed by bronchoprovocation with house dust mite allergen (*Dermatophagoides farinae*). In the antisense ODN-treated allergic rabbits there was a 55% improvement in dynamic compliance and a 61% reduction in bronchial hyperresponsiveness in response to histamine challenge (Fig. 4).

These findings suggest that adenosine is an important mediator of both airway obstruction and inflammation, and that some portion of these effects are mediated through the pulmonary adenosine A_1 receptor in the asthmatic lung. They further indicate that the lung may have great potential as a target for antisense ODN-based disease intervention in asthma and related lung pathologies. □

Methods

Preparation of allergic rabbits. Neonatal New Zealand white Pasturella-free rabbit littermates were immunized intraperitoneally within 24 h of birth with 312 antigen units per 0.5 ml house dust mite (*D. farinae*) extract (Berkeley Biologicals) mixed with 10% kaolin[23,26]. Immunizations were repeated weekly for the first month and then every 2 weeks for the next 3 months. At 4 months of age, sensitized rabbits were prepared for aerosol administration[25].

Synthesis and design of antisense ODNs. Phosphorothioate ODNs were synthesized on an Applied Biosystems model 396 oligonucleotide synthesizer using tetraethylthiuram in acetonitrile as sulphurizing agent. Crude ODNs (trityl on) were purified using NENSORB chromatography (DuPont). The

sequence of A1AS was: 5′-GATGGAGGGCGGCATGGCGGG-3′. Two different mismatched ODNs were used as controls and had the sequences: A_1MM 5′-GTAGGTGGCGGGCAAGGCGGG-3′, and A_1MM2 5′-GATGGAGGCGGG-CATGGCGGG-3′. Sequence of B_2AS: 5′-GGTGATGTTGAGCATTTCGGC-3′; sequence of B_2MM: 5′-GGTGAT TTGAGGATTTCGGC-3′.

Administration of aerosolized antisense ODNs and assessment of pulmonary function. Aerosols of either adenosine (0–20 mg ml^{-1}) or antisense or mismatch ODNs (5 mg ml^{-1}) were generated by an ultrasonic nebulizer (Model 646, DeVilbiliss, Somerset, PA), producing aerosol droplets of which 80% were less than 5 μm in diameter. Aerosols were administered directly to the lungs through an intratracheal tube. Rabbits were selected at random, and on day 1 pretreatment values for PC_{50} were obtained for aerosolized adenosine challenge. Animals were subsequently administered aerosolized antisense or mismatch ODN through the intratracheal tube (5 mg in a volume of 1.0 ml), for 2 min, twice daily for 2 days (total dose, 20 mg). On the morning of the third day, post-treatment PC_{50} values were recorded (post-treatment challenge). For Fig. 1, $N = 7$ for mismatch control A_1MM; $N = 4$ for mismatch control A_1MM2; and $N = 8$ for A_1AS antisense ODN. A_1MM2 ODN-treated animals ($N = 4$) were analysed separately and were not part of the crossover experiment. In 6 of the 8 animals treated with antisense ODN and reported in Fig. 1, a PC_{50} value for adenosine could not be obtained up to the limit of solubility of adenosine, 20 mg ml^{-1}. For the purpose of calculation, PC_{50} values for these animals were set at 20 mg ml^{-1}. The values given therefore represent a minimum figure for antisense effectiveness; actual effectiveness was higher. Other groups of allergic rabbits ($N = 4$–6 for each group) were administered doses of 0.5 or 0.05 mg A_1AS or A_1MM in the manner and according to the schedule described above (total doses of 2.0 or 0.2 mg). A_1AS reduced sensitivity to applied adenosine in a dose-dependent manner over the dose range of 0.2 mg total dose (PC_{50} adenosine, 8.32 ± 7.2 mg), 2.0 mg total dose (PC_{50} adenosine 14.0 ± 2.7 mg), and 20 mg total dose (PC_{50} adenosine, 19.5 ± 0.34 mg). No change in PC_{50} adenosine values occurred in rabbits treated with A_1MM control ODN over the same dose range (PC_{50} adenosine, 2.51 ± 0.46 mg at 0.2 mg A_1MM; 3.13 ± 0.71 mg at 2.0 mg A_1MM; and 3.25 ± 0.34 mg at 20 mg A_1MM). Assessment of bronchial hyperresponsiveness using histamine aerosol (Fig. 4) was performed as previously described[25].

Receptor binding. Airway smooth-muscle tissue from tertiary bronchi of rabbits ($N = 4$–6 per group) administered 0.2, 2.0 or 20 mg A_1AS, A_1MM, B_2AS or B_2MM in four divided doses over 48 h was assessed for receptor content[12,26,27]. Protein content was determined as described[28]. No significant inter- or intra-group difference in adenosine A_2 receptor-specific [^{3}H]CGS-21680 binding was observed in airway smooth-muscle plasma membranes isolated from A_1AS-treated animals (specific binding of 2,125 ± 371 c.p.m. per mg protein at 0.2 mg A_1AS; 1,925 ± 370 c.p.m. per mg protein at 0.2 mg A_1AS; and 1,861 ± 281 c.p.m. per mg protein at 0.2 mg A_1AS); from A_1MM-treated animals (specific binding of 2,210 ± 395 c.p.m. per mg protein at 0.2 mg A_1MM; 2,010 ± 390 c.p.m. per mg protein at 0.2 mg A_1MM; and 1,731 ± 276 c.p.m. per mg protein at 0.2 mg A_1MM); from B_2AS-treated animals (specific binding of 2,015 ± 225 c.p.m. per mg protein at 0.2 mg B_2AS; 1,910 ± 342 c.p.m. per mg protein at 0.2 mg B_2AS; and 1,776 ± 349 c.p.m. per mg protein at 0.2 mg B_2AS); or from B_2MM-treated animals (specific binding of 1,914 ± 192 c.p.m. per mg protein at 0.2 mg B_2MM; 1,875 ± 316 c.p.m. per mg protein at 0.2 mg B_2MM; and 1,805 ± 327 c.p.m. per mg protein at 0.2 mg B_2MM). Statistical significance was assessed by repeated measures analysis of variance (ANOVA), and Tukey's *t*-test.

Received 28 October; accepted 17 December 1996.

1. Weiss, K. B., Gergen, P. J. & Hodgson, T. A. *New Engl. J. Med.* **326,** 862–866 (1992).
2. *MMWR-Morbidity and Mortality Weekly Report* **41,** 733–735 (1992).
3. Chan-Yeung, M. & Malo, J. L. *Eur. Respir. J.* **7,** 346–371 (1994).
4. Pauwels, R. A., Kips, J. C. & Joos, G. F. *Clin. Exp. Allergy* **21** (suppl.), 48–55 (1991).
5. Bjorck, T., Gustafsson, L. E. & Dahlen, S. E. *Am. Rev. Respir. Dis.* **145,** 1087–1091 (1992).
6. Church, M. K. & Holgate, S. T. *Trends Pharmacol. Sci.* **7,** 49–50 (1986).
7. Cushley, M. J., Tattersfield, A. E. & Holgate, S. T. *Br. J. Clin. Pharmacol.* **15,** 161–165 (1983).
8. Holgate, S. T., Church, M. K. & Polosa, R. *Ann. NY Acad. Sci.* **629,** 227–236 (1991).
9. Driver, A. G., Kukoly, C. A., Ali, S. & Mustafa, S. J. *Am. Rev. Respir. Dis.* **148,** 91–97 (1993).
10. Pauwels, R. A. & Joos, G. F. *Arch. Int. Pharmacodyn. Ther.* **329,** 151–160 (1995).
11. Ali, S., Mustafa, S. J. & Metzger, W. J. *Agents Actions* **37,** 165–176 (1992).
12. Ali, S., Mustafa, S. J. & Metzger, W. J. *J. Pharmacol. Exp. Ther.* **268,** 1328–1334 (1994).
13. Ali, S., Mustafa, S. J. & Metzger, W. J. *Am. J. Physiol.* **266,** L271–L277 (1994).
14. Cushley, M. J., Tattersfield, A. E. & Holgate, S. T. *Am. Rev. Respir. Dis.* **129,** 380–384 (1984).
15. Mann, J. S. & Holgate, S. T. *Br. J. Clin. Pharmacol.* **19,** 685–692 (1985).
16. Wagner, R. W. *Nature* **372,** 333–335 (1994).
17. Stein, C. A. & Narayanan, R. *Curr. Opin. Oncol.* **6,** 587–594 (1994).
18. Bennett, C. F., Chiang, M. Y., Chan, H., Shoemaker, J. E. & Mirabelli, C. K. *Mol. Pharmacol.* **41,** 1023–1033 (1992).
19. Saijo, Y., Perlaky, L., Wang, H. & Busch, H. *Oncol. Res.* **6,** 243–249 (1994).
20. Ross, G. F. *et al. Hum. Gene Ther.* **6,** 31–40 (1995).
21. Pison, U., Neuendank, M. A., Weissbach, S. & Pietschmann, S. *Eur. J. Clin. Invest.* **24,** 586–599 (1994).
22. Hulsmann, A. R., Raatgeep, H. R., Saxena, P. R., Kerrebijn, K. F. & de Tongate, J. C. M. *J. Respir. Crit. Care Med.* **150,** 1012–1018 (1994).
23. Tsukagoshi, H., Haddad, E. B., Barnes, P. J. & Chung, G. F. *J. Pharmacol. Exp. Ther.* **273,** 1257–1263 (1995).
24. Feletou, M. *et al. Eur. J. Pharmacol.* **274,** 57–64 (1995).
25. Metzger, W. J. in *Late Phase Allergic Reactions* (ed. Dorsch, W.) 347–362 (CRC Press, Boca Raton, FL, 1990).
26. Jarvis, M. F. *et al. J. Pharmacol. Exp. Ther.* **251,** 888–893 (1989).
27. Trifilieff, A., DaSilva, A., Landry, Y. & Gles, J. P. *J. Pharmacol. Exp. Ther.* **263,** 1377–1382 (1992).
28. Bradford, M. M. *Anal. Biochem.* **72,** 240–254 (1976).

Acknowledgements. We thank C. Welch, L. Gregg, C. Knox, S. Police, S. A. Leonard and V. A. Best for technical assistance.

Correspondence and requests for materials should be addressed to J.W.N. (e-mail: 104130.440@compuserve.com).

Mechanism of odorant adaptation in the olfactory receptor cell

Takashi Kurahashi* & Anna Menini†

** National Institute for Physiological Sciences, Myodaiji, Okazaki 444, Japan, and Department of Biology, Osaka University, Toyonaka 560, Japan*
† Istituto di Cibernetica e Biofisica, Consiglio Nazionale delle Ricerche, 16149 Genova, Italy

Adaptation to odorants begins at the level of sensory receptor cells[1–5], presumably through modulation of their transduction machinery. The olfactory signal transduction involves the activation of the adenylyl cyclase/cyclic AMP second messenger system which leads to the sequential opening of cAMP-gated channels and Ca^{2+}-activated chloride ion channels[4–7]. Several reports of results obtained from *in vitro* preparations describe the possible molecular mechanisms involved in odorant adaptation; namely, ordorant receptor phosphorylation[8,9], activation of phosphodiesterase[10], and ion channel regulation[11–14]. However, it is still unknown whether these putative mechanisms work in the intact olfactory receptor cell. Here we investigate the nature of the adaptational mechanism in intact olfactory cells by using a combination of odorant stimulation and caged cAMP photolysis[15] which produces current responses that bypass the early stages of signal transduction (involving the receptor, G protein and adenylyl cyclase). Odorant- and cAMP-induced responses showed the same adaptation in a Ca^{2+}-dependent manner, indicating that adaptation occurs entirely downstream of the cyclase. Moreover, we show that phosphodiesterase activity remains constant during adaptation and that an affinity change of the cAMP-gated channel for ligands accounts well for our results. We conclude that the principal mechanism underlying odorant adaptation is actually a modulation of the cAMP-gated channel by Ca^{2+} feedback.

We investigated adaptation to odorant stimuli in single, dissociated olfactory receptor cells using whole-cell recording. An odorant pulse was applied to the cell and followed by a second pulse of the same intensity and duration (Fig. 1a). As reported previously[2], the peak amplitude of the response to the second pulse was small for short interpulse intervals but recovered as the interpulse interval increased.

When double-pulse experiments were repeated at +100 mV, or in a solution of low Ca^{2+} concentration at −50 mV, there was no significant difference between the first and second response to odorants (data not shown), indicating that Ca^{2+} entering the cell